Bioorganic Chemistry 116 (2021) 105313

Contents lists available at ScienceDirect

Bioorganic Chemistry

journal homepage: www.elsevier.com/locate/bioorg

Design, synthesis, and evaluation of HIV-1 entry inhibitors based on broadly neutralizing antibody 447-52D and gp120 V3loop interactions

Jagadeesh Senapathi [a,1], Akhila Bommakanti [a,1], Srinivas Vangara [b], Anand K. Kondapi [a,*]

[a] Dept. of Biotechnology and Bioinformatics, School of Life Sciences, University of Hyderabad, India
[b] School of Chemistry, University of Hyderabad, Hyderabad 500046, India

ARTICLE INFO

Keyword:
HIV-1
V3 loop
CCR5
Entry inhibitors
Drug design
Potent broadly neutralizing human monoclonal antibody
447-52D
1,3,5-triazine
Sulphonic acid
Isoniazid
Quinazolinone

ABSTRACT

The third variable loop region (V3 loop) on gp120 plays an important role in cellular entry of HIV-1. Its interaction with the cellular CD4 and coreceptors is an important hallmark in facilitating the bridging by gp41 and subsequent fusion of membranes for transfer of viral genetic material. Further, the virus phenotype determines the cell tropism via respective co– receptor binding. Thus, coreceptor binding motif of envelope is considered to be a potent anti-viral drug target for viral entry inhibition. However, its high variability in sequence is the major hurdle for developing inhibitors targeting the region. In this study, we have used an *in silico* Virtual Screening and "Fragment-based" method to design small molecules based on the gp120 V3 loop interactions with a potent broadly neutralizing human monoclonal antibody, 447-52D. From the *in silico* analysis a potent scaffold, 1,3,5-triazine was identified for further development. Derivatives of 1,3,5-triazine with specific functional groups were designed and synthesized keeping the interaction with co-receptor intact. Finally, preliminary evaluation of molecules for HIV-1 inhibition on two different virus strains (clade C, clade B) yielded IC50 < 5.0 μM. The approach used to design molecules based on broadly neutralizing antibody, was useful for development of target specific potent antiviral agents to prevent HIV entry. The study reported promising inhibitors that could be further developed and studied.

1. Introduction

HIV-1 Entry is facilitated by the interactions between the viral envelope protein (gp120) and host cell receptors and co-receptors involving conserved (C1-C5) and variable (V1-V5) regions of envelope [1]. The molecular analysis of interactions revealed that some of these regions were sufficiently exposed from the viral spike to generate neutralizing antibodies and participate in the interaction with small molecule inhibitors. The glycosylation of envelope protein (gp120 and gp41) varies in different virus strains and may contribute to the generation of strain-specific antibodies in the serum of HIV-1 infected individuals [2]. Most of these antibodies recognize the third hypervariable (V3) loop of gp120, especially *T*-cell line adapted strains of HIV-1 [3]. The loop contains 35 residues with an overall positive charge in the range of +2 to +10, which participates in the interactions with negative charge tyrosine sulphonate ($-SO_3^-$) group of CCR5 *N*-terminal [4]. V3 loop is further classified structurally into three areas: a base, stem, and crown [5]. The base part contains the most conserved residues located at the core of gp120 with disulfide bridges followed by the highly flexible stem and crown that extends outside of gp120 core when the loop is conformationally open [6]. The conserved residues in the crown region are immunogenic and also provide interactions with the CCR5-ECL2 loop [7]. High immunogenicity of the V3 loop has been widely exploited to develop synthetic mimics to act as an efficient antigen to produce antibodies in the immunization process [8]. X-ray crystallography studies disclosed that the crown part of the V3 loop adopts β- hairpin conformation in both V3 loop-containing gp120 core and antibody-V3 loop complex. This is assumed to be because of a conserved region in the centre of the crown consisting of GPXR epitope (GPGR in subtype B and GPGQ in subtypes A, C, and D), which preserves the structural elements in the V3 loop irrespective of sequence variability in other portions of V3 loop [9]. Although most anti V3 -loop antibodies neutralize only a few strains, some of them neutralize diverse strains of the virus. The V3 loop native conformation can elicit anti-V3 broadly neutralizing antibodies like 447-52D and 2219, interacting with other immunodominant regions on gp120 [10]. This study explores the

* Corresponding author.
E-mail address: akondapi@uohyd.ac.in (A.K. Kondapi).
[1] Authors have contributed equally to the work presented in this paper.

https://doi.org/10.1016/j.bioorg.2021.105313
Received 4 July 2021; Received in revised form 25 August 2021; Accepted 27 August 2021
Available online 30 August 2021

antibody 447-52D to derive entry inhibitors based on its interaction with gp120 V3 loop. Previous studies of 447-52D show contact with both stem and tip of the V3 loop to neutralize the subtype B virus (Fig. 1). From the crystal structure analysis, 447-52D mAb CDRH3 C-terminal interacts with V3 crown N -terminal via main chain interactions and side chains interactions at V3 tip residues (Fig. 1**)** [11].

Interaction stability was explained by:

i. The anionic (AspH95 of the Ab) and cationic (V3 loop Arg315) residues formed the Salt bridge.
ii. The antibody aromatic residues (TyrH100J and TrpH33 of the 447-52D heavy chain) formed π-cation stacking with cationic (Arg315 of V3 loop).
iii. Van der Waals interaction between V3 loop residues (Pro313 of V3 loop - TrpL91 and V3 loop -TrpL96).
iv. Water-mediated hydrogen bond network at the antigen-binding site [12].

These interactions were used as a basis for design of small molecules that can mimic the binding of the antibody to gp120 and subsequently blocking viral entry. The neutralizing antibody interactions provide knowledge about valid target site recognition and the compounds designed to target these sites are expected to modulate the protein–-protein interactions [13]. The mimicking chemosuperiors are considering as "hits" for lead molecule development with various modifications. The small molecule design is based on the structural consideration of drug-like molecules based on pharmacological stability, conformational changes, and reduced metabolism [14]. In this paper, we report the design, synthesis, characterization, and evaluation of promising molecules those mimic the antibody-V3 loop interaction and block HIV-1 entry.

2. Results and discussion

2.1. In silico design and development of 447-52D mimetics

Pep:MMs:MIMIC server was used to obtain hits based on the 447-52D and V3 loop interaction as described. The interacting interface and V3 loop sequence submitted to pep:MMs:MIMIC server led to the development of a pharmacophore used to screen the MMsINC database of small molecules to return hits. Two hundred small molecules were reported and scored, based on the match to the pharmacophore. Top 30 molecules are presented along with scores in (**Table S1)**. The molecules reported by pep:MMs:MIMIC were docked with the V3 loop structure (PDB Id:1Q1J) using GOLD by the protocol described to build a ranked hit library to obtain molecules with high scores and better interactions. The top 20 molecules (**Table S2a**) from the hit library were docked to whole structure of gp120 (PDB ID:2B4C). The amino acid residues, Arg306 and Lys307, were seen to be involved in the interaction with most molecules. These residues were also crucial in the interaction interface of 447-52D and V3 loop. Apart from these residues, Cys297 and Cys331 were also important for the interaction. Based on the number, type, other parameters of interactions and the docking score, ten molecules (**Table S2b)** were selected for further development. The selected molecules are given in Fig. 2. These molecules led to identifying a core structure, s-triazane or 1,3,5-triazine, the sub-structure reported to be present molecules with broad spectrum activities including antimicrobial, anticancer, tumour growth inhibition and estrogen receptor modulators [15]. This sub-structure was further developed, molecules were synthesized, and validated using activity studies viz. inhibition of HIV-1 entry and HIV-1 replication.

2.2. Chemistry

Development of molecules from the selected hits was based mainly on the significant pharmacophore features of the parent structure. Molecule UHLMTA-A9 type, has been previously reported (see Fig. 3) to inhibit HIV-1 infection [16] and hence, this molecule was considered for

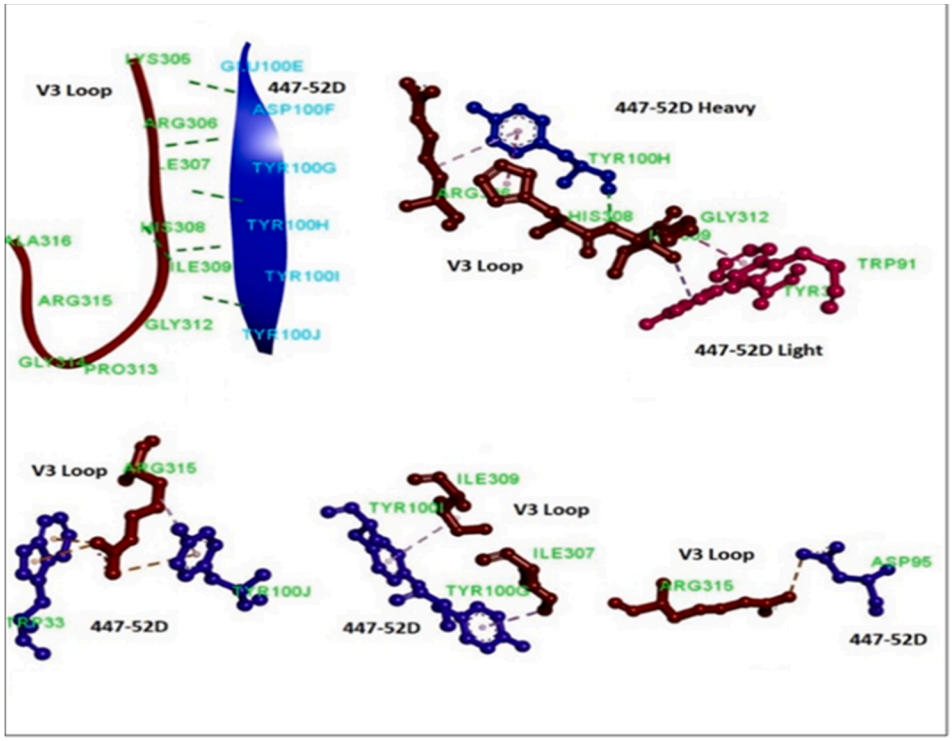

Fig. 1. The interaction interface between 447-52D and HIV-1 gp120 V3 loop.

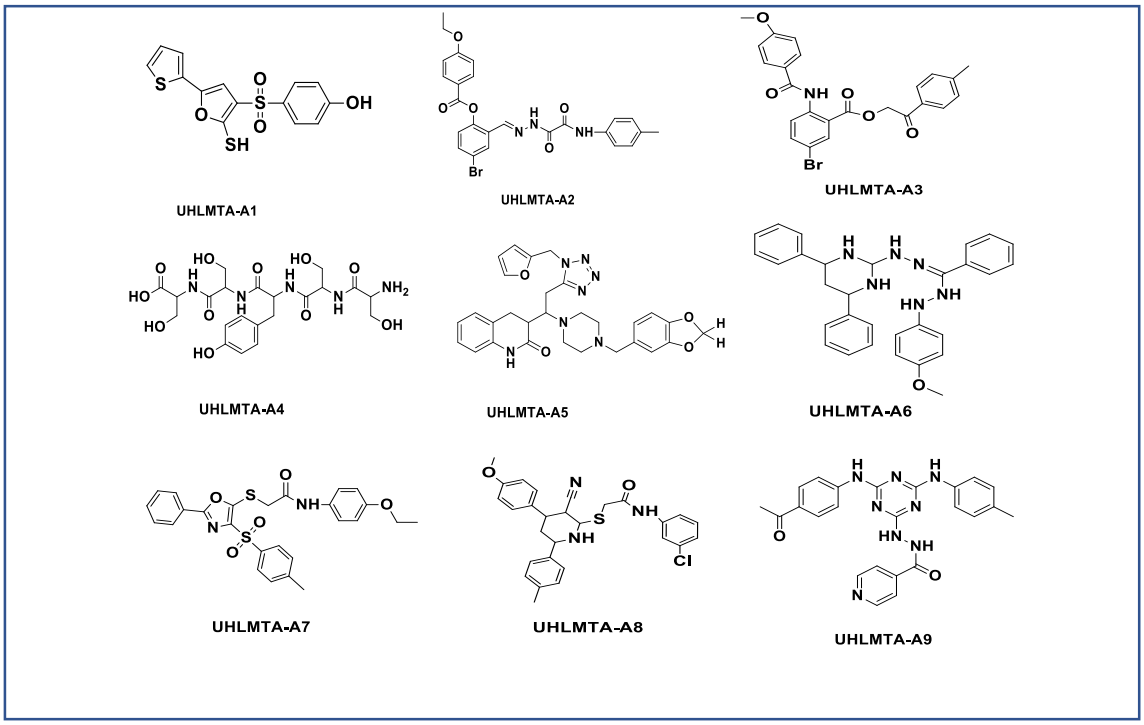

Fig. 2. Top nine molecules selected from the virtual screening protocol for 447-52D mimics.

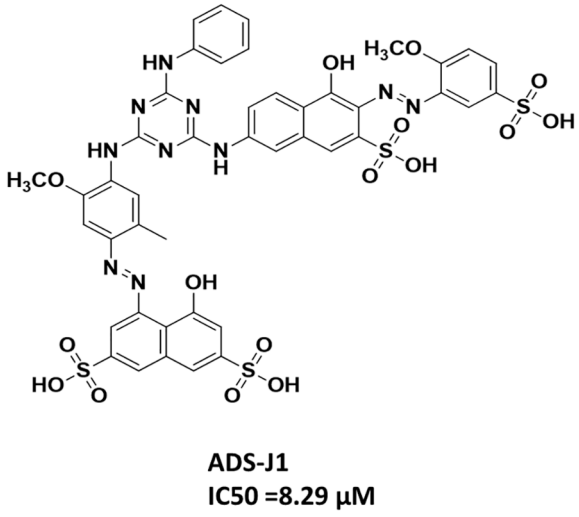

Fig. 3. Chemical structures of HIV entry inhibitor targeting gp41.

further development. The 1,3,5-triazine skeleton of the UHLMT-A9 molecule is mainly substituted with different functional groups to design new derivatives (Table 1**)** with synthetic ease as described by the below methodology. The functional groups that could mimic interactions of the V3 loop with co-receptor CCR5 were considered for substitution to facilitate competitive binding with the loop, conferring blocking interaction with the co-receptor [17]. The V3 loop-CCR5 participates principally through ionic interactions involving the positively charged V3 region and negatively charged sulfate group of CCR5. However, the sulphonate group mediated interactions alone may not be sufficient to inhibit entry inhibition [18]. We developed molecules containing electron abundant negative charge moieties for participation in hydrophilic, hydrophobic, and cation -π stacking type interactions with V3 loop residues. The designed analogues of UHLMT-A9 contains negative charge sulfonate groups, substituted benzene ring, quinazolinone, isoniazid, and other functional groups. The 1,3,5-triazine scaffolds were synthesized by substitution of less expensive cyanuric chloride with different functional groups. The synthesis was carried out mainly through nucleophilic substitutions and coupling reaction mechanisms in alkali conditions. The sequential ring substitution was majorly depending on reaction time and temperature [19]. The cyanuric chloride reaction with different aromatic amines to replace chlorides on 1,3,5-triazine ring with amino groups to form mono, di, tri substituted - s-triazines (Schemes 2–4). The substitution of the chlorine atom depends on the reaction conditions indicated therein. The substituted groups on 1,3,5-triazine create structural advantage for strong interactions at target site.

The target compounds **7a-c** were prepared as per the procedure in Scheme 2**.** The **6a-c** arylamines were used for substitution of single chloride on s-triazine to form corresponding molecules (**7a-c).** The whole reaction was controlled under low temperature < 5 °C and the slow addition of aq. NaOH, which was acting as neutralizing agent for released HCl during reaction [20].

For the synthesis of **UHLMTJ-257a-c,** the second chloride of monochloride substituted **7a-c** molecules replaced with isoniazid, in the presence of aq. NaOH between pH 7.5 to 8.0 under room temperature (RT) in Scheme 3 [21]. However, **UHLMTJ-259a-c** were synthesized through nucleophilic substitution of chloride with 2-(4-aminophenyl)-2,3-dihydro-1H-quinazolin-4-one **(4)** which is prepared as per the Scheme 1 [22,23]. The reaction was carried out at overnight under inert conditions in the presence of K_2CO_3 that was shown in Scheme 4**.**

The synthetic route for the preparation of trichloro substituted 1,3,5-triazine molecules **(UHLMTJ-258a-c, 260a-c, 261a-c)** was explained in Schemes 3 and 4**.** The third chloride replacement was difficult due to less availability of chlorides on 1,3,5-triazine. So, the reaction was carried in excess equivalent of corresponding arylamines at a high temperature (110 °C). In that, the excess amine itself is acting as a base to neutralize the reaction. While excess P-toluidine was treated with **UHLMTJ-257a-c** and **UHLMTJ-259a-c** to form **UHLMTJ-258a-c,** and **UHLMTJ-260a-c,** respectively. Compounds **UHLMTJ-261a-c** were prepared as per the Scheme 4 and excess of isoniazid was treated with **UHLMTJ-259a-c** to get desired molecules [24].

Table 1
The newly designed and synthesized analogues of 1,3,5-triazine.

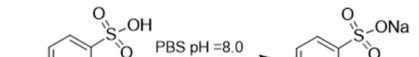

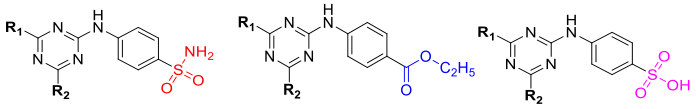

R_1	R_2	Compound Code		
-Cl	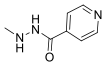	UHLMTJ-257a	UHLMTJ-257b	UHLMTJ-257c
	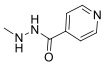	UHLMTJ-258a	UHLMTJ-258b	UHLMTJ-258c
-Cl	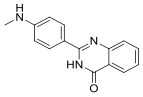	UHLMTJ-259a	UHLMTJ-259b	UHLMTJ-259c
	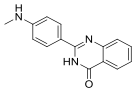	UHLMTJ-260a	UHLMTJ-260b	UHLMTJ-260c
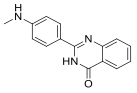	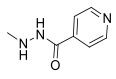	UHLMTJ-261a	UHLMTJ-261b	UHLMTJ-261c

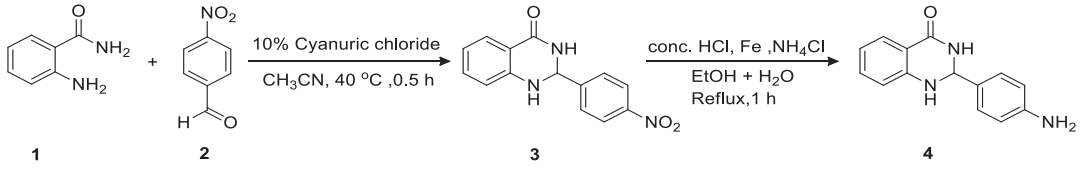

Scheme 1.

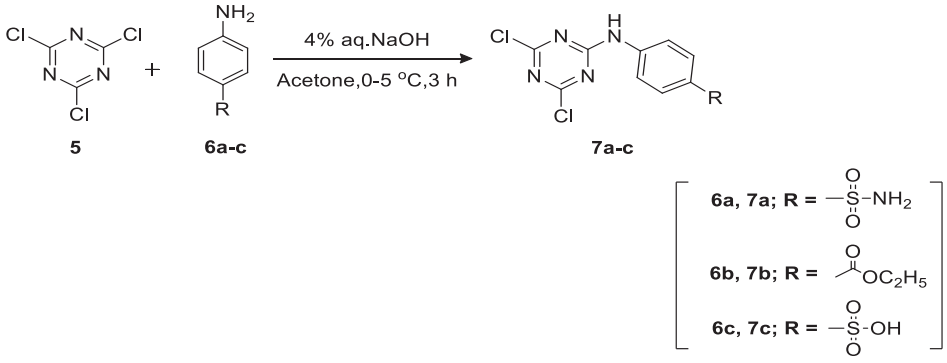

Scheme 2.

The experimental observation concluded that following order essential for chloride atom substitution. As per that first electron-withdrawing groups contained amines and then bulky size amines, followed by small, and electron-rich amines. All substituted compounds were further purified by washing, recrystallized, and characterized by NMR, IR, and HRMS. The yield and melting points of molecules are reported with spectral data. The yield of sulfonic acid derivates was significantly low compared to others. Here, we prepared sodium salt of sulfonic acid by dissolving sulfonic acid groups contained molecules in PBS buffer at pH 8.0. The hydrogen ion was replaced by sodium ion to form the sodium salt of sulfonic acid confirmed by molecular solubility.

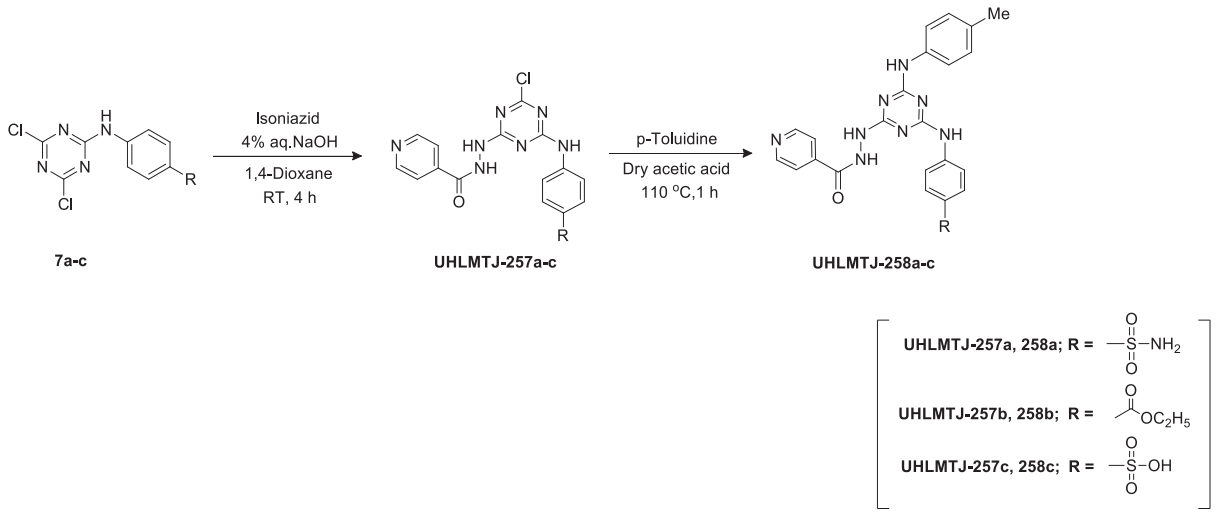

Scheme 3.

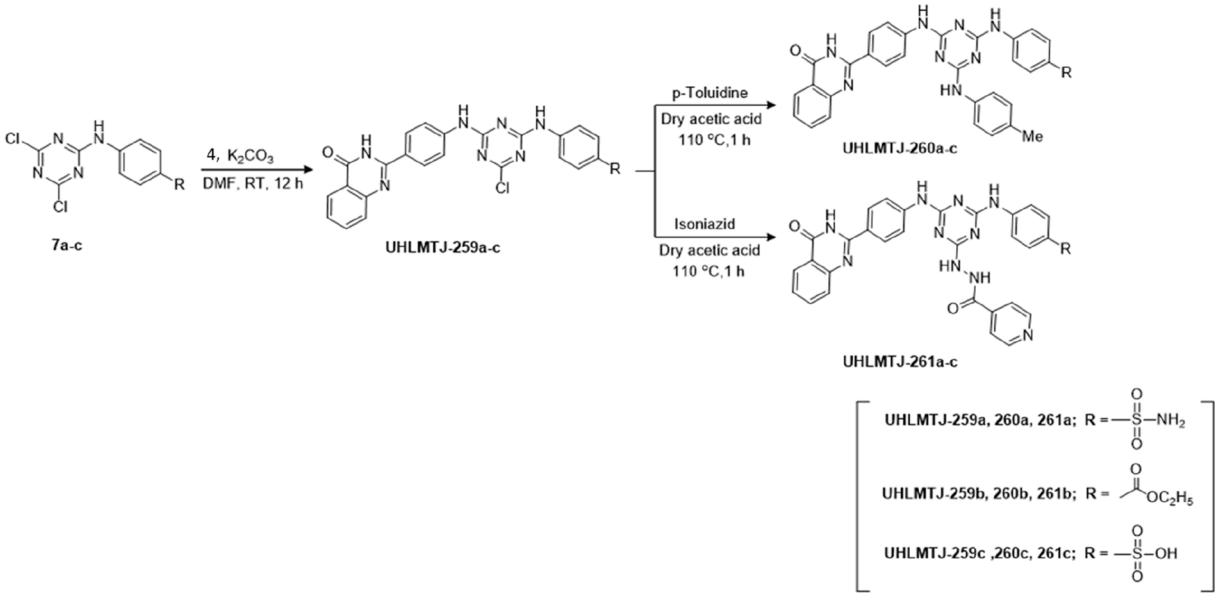

Scheme 4.

2.3. Structural dynamics of gp120-V3 loop

Number of studies have reported that the recognition of gp120 binding regions by small molecules is dependent on the V3 structural dynamics as some molecules recognize CD4 bound open loop gp120 structure while some recognize the native closed structures better [25]. To understand this, the selected molecules were docked with the open, and closed structures of gp120 and the binding energies were analysed to understand the mode of action of the compounds. The structure of the gp120, complexed with CD4 and X5 antibody, retrieved from RCSB PDB (PDB ID: 2B4C) has an open loop structure which was used for docking. To obtain a closed loop structure of gp120, the crystal structure was subjected to MD simulation for 20 ns **(Fig. S1).** The Carbon backbone of the structure before and after simulation was overlapped to monitor the structural changes **(Fig. S2).** Major structural change was seen in the V3 loop of the gp120 structure, where an open structure seen when complexed with CD4 was changed to a closed structure when subjected to the molecular dynamics protocol. This change in conformation between CD4 bound and unbound gp120 has been reported in several studies [26].

2.4. In silico binding studies of 1,3,5-traizine derivatives

Analysis of the molecular docking scores of 1,3,5-traizine derivatives between the open and closed loop conformation of gp120 showed better affinity with closed structures than open structures in the mimetics **(**Table 1**).** From the docking scores and the interacting residues, it was observed that the binding region for 447-52D mimetics was similar to the antibody interacting interface. Electrostatic interactions, Hydrogen bonding and cation-π interactions were observed in the binding of the compounds, while electrostatic interactions were dominant. The compounds designed to possess an overall negative charge tend to interact with greater affinity due to the dominant positive charge of the V3 loop. It was observed that Trichloro substituted molecules showed better binding, than dichloro substituted molecules. Further, moieties with aromatic and anionic properties such as quinazolinone, sulphonate, sulphanilamide and isoniazid substituted molecules have shown better binding energies computation from Autodock. Moieties such as quinazolinone ring (—NH—C═O), sulfonate ($—SO_3^-$), safinamide ($—SO_2NH_2$), and ester groups ($—COOC_2H_5$) interact with side chains of

the crown (HIS308, ILE309, GLY312, PRO313, TYR318), stem (THR 297, PRO299, ARG304) regions to form hydrogen bonds. Along with those interactions, the quinazolinone, isoniazid and s-triazine aromatic rings were also involved in cation -π stacking at the base part of the V3 loop **(**Fig. 4**).** The binding region also included amino acids from the base of the V3 loop in closed structures, most prominent being Asn332, Thr297 and Asn295. This was also reflected in preference of 447-52D mimetics to choose closed structure where the stem, crown, and base of the V3 loop and other surrounding regions of gp120 were in proximity, due to the folded V3 conformation. Among various residues outside V3 loop involved in the binding were Arg444, Thr413, Val292, Lys337 in the closed loop conformation.

2.5. Cell cytotoxicity (MTT Assay) of selected molecules

The cytotoxicity of the newly designed and synthesized drug-like molecules on human cell line Sup-T1 cells was conducted in the presence of increasing concentrations, 50, 100, 250, 500 and 750 μM, and the cell viability was evaluated using MTT assay. The results of analysis of 50% cell survival concentrations (CC50) showed that the molecules containing sulfonic groups (UHLMTJ-257c, 258c, 259c, 260c, 261c) exhibited significant toxicity than the molecules devoid of sulfonic group (UHLMTJ-257a, b etc.,). Along with quinazolinone, isoniazid combination with sulphnamide and sulfonic group molecules, UHLMTJ-260c, 261a, 261c, were more toxic and CC_{50} was <200.0 μM. The remaing molecules were modarately toxic at concertation > 300 μM, the dose-dependent cytotoxicity is depicted in Fig. 5 and CC_{50} values are presented in Table 2**.**

2.6. Anti-HIV-1 activity (p24 Assay) of molecules

The antiviral activity of the molecules was analysed against HIV-1 replication in SupT1 cells. SupT1 cells were challenged with HIV-1 using 93IN101 (Clade C) and NL4-3 (Clade B) virus in the presence of increasing concentrations (0.5–10 μM) of the compounds. The virus replicated was estimated by measuring the p24 capsid protein in the infected cells using p24 antigen capture assay, the results are presented in Fig. 6 and IC_{50} values are presented in Table 2. Tri chloro substituted compounds showed better anti-HIV-1 activity than di chloro substitution of corresponding molecules. Among these quinazolinone, isoniazid combination with sulfonic and sulphonamide contained molecules UHLMTJ-258c, 259c, 260a, 260c, 261a, 261b, 261c, were highly active with IC_{50} of <2.0 μM on both clades of virus. This difference could be attributed to the differences in interaction and affinity with V3 loop as seen in the results of the *in silico* analysis. These molecules showed similar anti-HIV-1 activity against both clade C and clade B type of virus, while relatively better activity exhibited against clade B.

2.7. Inhibition of gp120-mediated entry using dye transfer assay

Inhibition of gp120 mediated viral entry was tested by monitoring a cell-mediated fusion of envelope expressing HL2/3 and SupT1 cells. The compound **UHLMTJ-261c**, was tested for inhibition by dye redistribution assay as described. T-20 (Enfuvirtide) was used as a control and the compound were tested at respective IC_{80} concentrations in pre-incubation experiment, where the compounds were incubated with HL2/3 cells before co-culturing them with SupT1 at 1:1 ratio. The compound showed better blocking of entry, as seen in Fig. 7, with fewer fused cells (cyan coloured cells) in comparison to control cells.

3. Conclusion

We elaborate the design and development of small-molecule mimics based on interaction of broadly neutralizing antibody 447-52D with gp120 V3 loop. The 1,3,5-triazine scaffold of UHLMT-A9 molecules derivatives were designed and synthesized with different functional groups. The interaction studies of the derivatives disclosed that most of the interactions were hydrophilic along with hydrophobic and π -π stacking. Tri-substituted molecules interact effectively with better docking scores. The antiviral activity results suggested that all molecules have IC_{50} activity below 5.0 μM. This study has identified a promising molecular scaffold that can be further explored to obtain potent HIV-1 inhibitors targeting viral entry.

4. Experimental

4.1. Computational design of compounds from 447-52D-V3 loop interacting complex

The structure 1Q1J solved by Stanfield et al. with a resolution of 2.5 Å was the closest crystal structure record found, for the 447-52D-V3 loop complex. Pep:MMs:MIMIC server was used to screen the MMs database for molecules with desired physical properties of the 447-52D-V3 loop interaction interface. The V3 residues I309, I307, H308, R315 etc. were

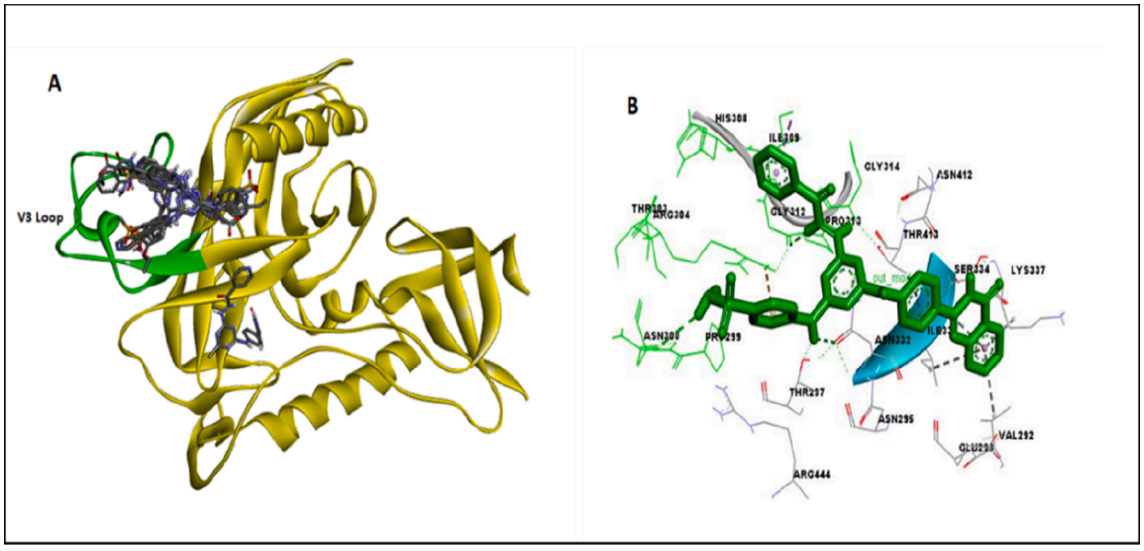

Fig. 4. A) Depicts the binding region of all molecules with gp120. The molecules can be seen bound in the interface of the folded V3 loop stem (green) and the base of the loop and surrounding residues (grey). B) Depicts the interface of the interaction of molecule UHLMTJ −261b with gp120.

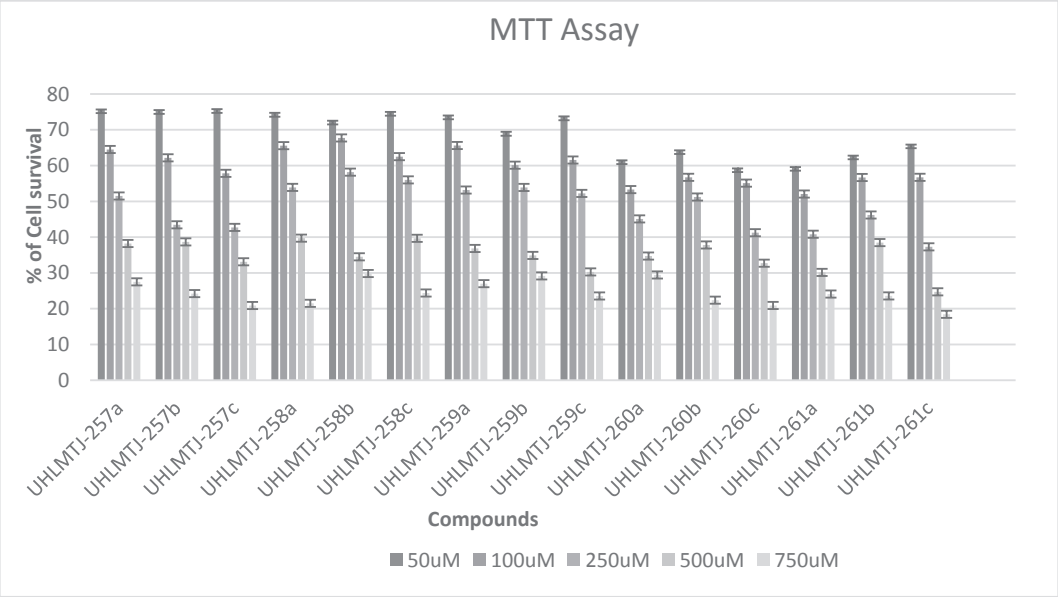

Fig. 5. Cytotoxicity of the compounds tested on SupT1 cell line. The toxicity was measured by MTT assay at increasing concentration of the compounds and the % cytotoxicity was plotted against the concentration. Mean ± SD was plotted. P value was ≤0.05.

Table 2
Binding energy (kcal/mol) in interaction with V3 loop, CC_{50}, IC50 and therapeutic index (TI) of newly synthesized compounds. (ND: Not determined).

S. No	Compound Code	Binding Energy (Kcal/mol)	CC50 (μM) (SupT1)	IC50 ± SD (μM) (93IN101, Clade C)	IC50 ± SD (μM) (NL4-3, Clade B)	TI (93IN101)	TI (NL4-3)
1	T20	ND	>100	0.035	0.028	>2000	>3000
2	UHLMTJ-257a	−7.3	>300	4.03 ± 0.15	3 ± 0.14	>74.44	>100.0
3	UHLMTJ-257b	−6.8	>300	4.50 ± 0.18	3.3 ± 0.15	>66.66	>90.90
4	UHLMTJ-257c	−7.7	272.47	3.25 ± 0.12	2.2 ± 0.18	83.83	123.85
5	UHLMTJ-258a	−8.0	>300	2.86 ± 0.15	2.1 ± 0.12	>104.89	>142.85
6	UHLMTJ-258b	−7.2	>300	3.60 ± 0.17	3.8 ± 0.19	>83.33	>78.94
7	UHLMTJ-258c	−8.7	>300	1.14 ± 0.09	1.0 ± 0.11	>263.15	>300.0
8	UHLMTJ-259a	−8.7	>300	2.16 ± 0.19	1.5 ± 0.2	>138.88	>200.0
9	UHLMTJ-259b	−8.3	>300	2.83 ± 0.12	2.5 ± 0.19	>106.00	>120.0
10	UHLMTJ-259c	−8.8	>300	1.54 ± 0.15	1.2 ± 0.13	>194.80	>250.0
11	UHLMTJ-260a	−9.5	209.28	1.74 ± 0.12	1.1 ± 0.15	120.27	190.25
12	UHLMTJ-260b	−8.5	267.29	2.31 ± 0.16	2.6 ± 0.12	115.70	102.80
13	UHLMTJ-260c	−9.4	176.02	0.94 ± 0.08	0.7 ± 0.04	187.25	251.45
14	UHLMTJ-261a	−10.5	151.69	0.76 ± 0.05	0.6 ± 0.03	199.59	252.81
15	UHLMTJ-261b	−9.0	244.22	1.93 ± 0.12	1.8 ± 0.1	126.53	135.67
16	UHLMTJ-261c	−9.6	186.86	0.52 ± 0.04	0.5 ± 0.06	359.34	373.72

given as the interacting residues. The scoring was based on both pharmacophoric (60%) and shape (40%) parameters. The molecules reported by Pep:MMs: MIMIC were further screened to obtain hits with good binding affinity to V3 loop. GOLD docking suite was used for screening of the reported molecules. The processed 1Q1J file was used as the receptor, and the docking was performed in batch. The binding site residue was specified as Arg315 and 5 Å was set as the radius of the cavity. Genetic algorithm was selected as the default program for exploring the conformational space for ligand binding. The parameters for GA run were set to default as described; 100 was set as the population size, the selection pressure was set to 1.1, the number of operations was given as 10,000, and one island and niche size of 2 was set per run. Mutation and cross over rates were set at 100. The GOLD score was used as a metric to score the molecules. The output was set to 10 solutions per molecule.

Further, Autodock Vina v1.2 was used to dock the selected, redesigned, synthesized, and tested molecules with X-Ray structure of gp120 obtained from PDB record (2B4C) and the minimized and processed structure of gp120.

4.2. Structural dynamics of gp120-V3 loop

The processed PDB structure of gp120 was subjected to molecular dynamics simulation using the GROMOS96 43a1 force field. The simulation was carried in water using the SPC/E water model and a cubic box was defined to build the system (protein in water). The protein was placed in the centre of the box, 1 nm from the edge. Thirteen water molecules in the solvent were replaced by negatively charged Chloride ions to balance the charge and neutralize the system. Before proceeding with the simulations, the structure was subjected to energy minimization using the Steepest Descent Algorithm with 50,000 iteration steps and a step size of 0.01 KCal/mol. The maximum force on the system was set to 1000 KJ/mol/nm, and the minimization would stop if the force fell below the level. The minimized system was equilibrated at constant pressure and constant volume for 200 ps each. The equilibrated system was subjected to final dynamic simulation for a 20 ns run. The simulated structure was evaluated by RMSD and radius of gyration. GROMACS 5.0 was used for setting up and running the MD simulation. The final structure obtained was used for further docking studies.

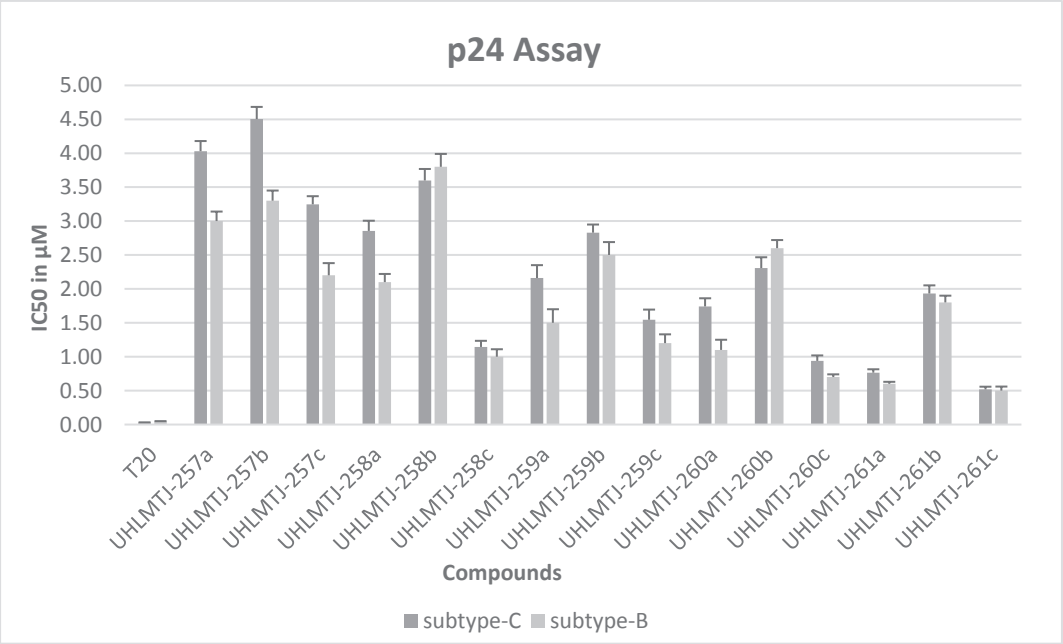

Fig. 6. Graphical representation of action of synthesized molecules against replication of HIV-1 subtype B (NL4-3) subtype C (93IN101) in IC_{50} value. Each data point is an average of three independent experiments and presented as Mean ± SD. T20 was used as a positive control.

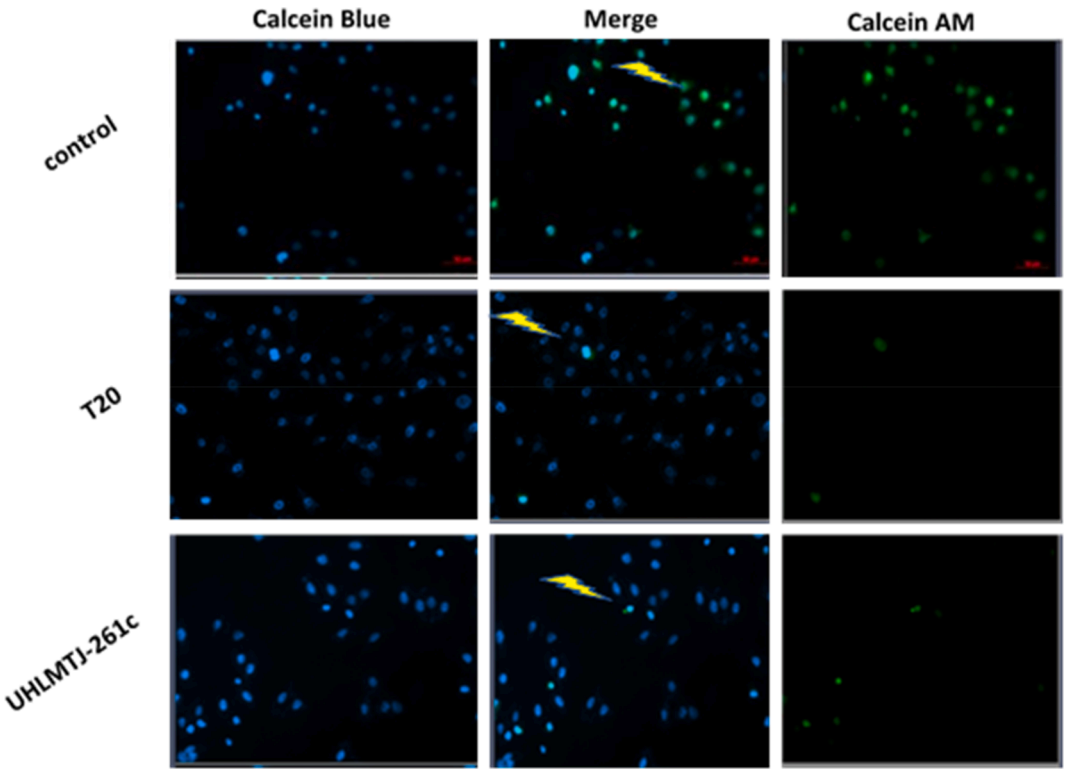

Fig. 7. Dye transfer assay to monitor inhibition of cell fusion in presence of compound UHLMTJ-261c. The images were captured by Leica Fluorescent Microscope as different regions of coverslip. Fusion in absence of compounds was considered as control and in presence of T-20 is considered positive control. Fused cells exhibit cyan color and are indicated by yellow flash for visualization.

4.3. Chemistry

4.3.1. General experimental information

All reagents and solvents were of analytical grade and were used without further purification. High precision instruments were used for molecular characterization. The structural characterization of synthesized molecules was confirmed by NMR (600 MHz), ESI- HRMS, FTIR and melting point apparat. The chemical shift value of compound peaks reported in ppm (δ scale) and coupling constant (J) vlaues were given in Hz and DMSO-d_6 were used as a standared solvent. The peaks multiplicity was explained in singlet (s), doublet (d), triplet (t), quartet (q), multiplet (m) and broad (br). The low solubility of compounds

restricted the ^{13}C NMR of the compounds. It was interesting to note, —N—H proton exchange in ^{1}H NMR of some compounds. Insilco studies was carried out by using Pep:MMs:MIMIC server, GOLD, GROMACS 5.0, Autodock Vina V1.2. The biological experiment were conducted by CO_2 Incubator, ELISA Plate reader, Fluorescent Microscope (Carl-Zeiss) and Bruker ImageJ Java 1.8.0_112. Graphpad Prism 6.0 was used for all statistical analysis.

4.3.2. Experimental procedures

4.3.2.1. Synthesis of 2-(4-aminophenyl)-2,3-dihydro-1H-quinazolin-4-one (4). The anthranilamide (0.73 mmol) was dissolved in 2 ml of acetonitrile, then mixed with 4-nitrobenzaldehyde (0.73 mmol) and cyanuric chloride (0.135 mmol, 10 mol %) at RT. The reaction mixture was reflexed at 70 °C for 0.5 h, and after the reaction was completed, the access solvent was evaporated and washed with cooled water to get a yellow solid (**2.8**) with a 95 % yield. The solid nitro, compound **2.8** (0.01 mol), was dissolved in a mixture of ethanol (10 ml), water (0.05 ml), and added few drops of a con. HCl. The solution was gently stirred for 10 min at room temperature and then added iron metal powder (0.03 mol) and NH_4Cl (0.03 mol). Finally, the total mixture was refluxed for 0.5 h at 60 °C. TLC was used for monitoring the completion of the reaction. After completing the reaction, the reaction mixture was cooled at RT and then neutralized with the aq.solution of 10% $NaHCO_3$, poured into cooled water, and filtered to get the solid supernatant cake, which was washed with hot ethanol and chloroform in 1: 1 ratio. To obtain the final compound, evaporate the solvent, and got the pure amino compound (**2.9**) with a 40% yield; no further purification was required.

Yield 40%. mp 202–204 °C. ^{1}H NMR (600 MHz, DMSO-d_6) δ 8.0 (brs, 1H, —N**H**—C═O), 7.58 (d, J = 6.6 Hz 1H, Ph—**H**), 7.18 (d, J = 7.2 Hz, 1H, Ph—**H**), 7.13 (d, J = 8.4 Hz, 1H, Ph—**H**) 6.84 (s, 1H, —N**H**), 6.72–6.60 (m, 3H, Ph—**H**), 6.54 (d, J = 7.8 Hz, 2H, Ph—**H**), 5.72 (d, J = 9.6 Hz, 1H, —NH—C**H**—NH), 5.55 (s, 1H, —N**H**$_2$). ^{13}C NMR (DMSO-d_6, 150.91 MHz) δ:164.46, 149.36, 148.87, 133.67, 128.76, 128.41, 127.88, 117.47, 115.48, 114.90, 114.03, 67.56 ppm. IR (neat):ν_{max}3287, 1607, 1557, 1487, 1408, 1329, 1176, 1126, 1033, 1007, 832, 800 cm^{-1}. HRMS (ESI): *m/z* [M+H]$^+$ Calcd for $C_{14}H_{11}N_3O$ 238.0980;Found, 238.0971.

4.3.2.2. General procedure for synthesis of the target compound (7a-c). The mixture of 2,4,6-trichloro -1,3,5-triazene (0.01 mol) and arylamine (0.01 mol) was taken in acetone and stirring at 0–5 °C. After 1 h, 4% of NaOH solution was added dropwise with rapid stirring and then continue the reaction up to 2 h. After completing the reaction, the mixture was poured into crushed ice and then neutralized with 2 M HCl under continuous stirring. The reaction mixture was filtered, washed with ice water, dried, and recrystallized in acetone.

4.3.2.2.1. 4-((4,6-dichloro-1,3,5-triazin-2-yl) amino) benzene sulphonamide (7a). Yield 92%. mp Infusible. ^{1}H NMR (600 MHz, DMSO-d_6) δ 11.39 (s, 1H, —N**H**), 7.79 (d, J = 6.0 Hz, 2H, Ph—**H**), 7.72 (d, J = 6.0 Hz, 2H, Ph—**H**), 7.73 (brs, 2H, —N**H**$_2$). ^{13}CNMR (DMSO-d_6, 150.91 MHz) δ:170.30, 169.52, 164.50, 140.51, 127.17, 121.63, 120.83 ppm. IR (neat): ν_{max} 3293, 3208, 1619, 1552, 1516, 1493, 1425, 1379, 1328, 1295, 1226, 1162, 1022, 900, 875, 845, 831 cm^{-1}. HRMS (ESI): *m/z* [M+H]$^+$ Calcd for $C_9H_7Cl_2N_5O_2S$, 319.9776; Found, 319.9766.

4.3.2.2.2. Ethyl 4-((4,6-dichloro-1,3,5-triazin-2-yl) amino) benzoate (7b). Yield 93%. mp > 300 °C. ^{1}H NMR (DMSO-d_6) δ 10.89 (s, 1H, —N**H**), 7.87 (d, 2H, Ph—**H**), 7.70 (d, 2H, Ph—**H**) 4.20 (q, 2H, —C**H**$_2$), 1.22 (t,3H, —C**H**$_3$).^{13}CNMR (DMSO-d_6, 150.91 MHz) δ: 165.79, 154.64, 142.27, 130.73, 125.48, 120.54, 61.08, 14.73 ppm. IR (neat): ν_{max} 3281, 3201, 1687, 1607, 1541, 1504, 1431, 1387, 1337, 1318, 1282, 1253, 1226, 1186, 1165, 1124, 1014, 960, 878, 836, 814 cm^{-1}.

4.3.2.2.3. 4-((4,6-dichloro-1,3,5-triazin-2-yl) amino) benzenesulfonic acid (7c). Yield 73%. mp Infusible. 1H NMR (600 MHz, DMSO-d_6) δ 11.16 (s, 1H, —N**H**), 7.58 (d, J = 8.4 Hz, 2H, Ph—H), 7.52 (d, J = 8.4 Hz, 2H, Ph—**H**). ^{13}C NMR (DMSO-d_6, 150.91 MHz) δ: 170.21, 169.30, 164.30, 144.72, 137.73, 126.74, 121.20 ppm. IR (neat): ν_{max} 3469, 3270, 1618, 1557, 1498, 1423, 1384, 1319, 1225, 1170, 1127, 1035, 1007, 962, 876, 846, 828 cm-1. HRMS (ESI): *m/z* [M+H]$^+$ Calcd for $C_9H_6Cl_2N_4O_3S$, 320.9616; Found, 320.9605.

4.3.2.3. General procedure for synthesis of the target compound (UHLMTJ-257 a-c). The monochloride substituted triazene **7a-c** (0.01 mol), and the corresponding arylamine (0.01 mol) were dissolved in 1,4- dioxane at RT. During the reaction, the released HCl was neutralized with dropwise added 4% of NaOH (Alternatively, dry DMF as a solvent and K_2CO_3 as a neutralizing agent also used) and continue reaction up to 3 h and maintained reaction mixture at pH 7.5–8.0. After completing the reaction, the total blend was neutralized, washed with excess water, filtered to get the recrystallized product in dry DMF.

4.3.2.3.1. 4-((4-chloro-6-(2-isonicotinoylhydrazinyl)-1,3,5-triazin-2-yl)amino)benzenesulphonamide (UHLMTJ-257a). Yield 85%**.** mp Infusible. ^{1}H NMR (600 MHz, DMSO-d_6): δ11.02 (d, 1H, —NH—N**H**—C═O), 10.65 (brs, 1H, —N**H**—NH—C═O), 10.34 (brs, 1H, —N**H**)**,** 8.85–8.76 (m, 4H, Ph—**H**, Py—**H**), 7.82–7.77 (m, 2H, Py—**H**), 7.76–7.09 (m, 2H, Ph—**H**), 7.22 (brs, 2H, —N**H**$_2$-S═O). IR (neat): ν_{max} 3206, 1555, 1514, 1408, 1327, 1189, 1154, 1100, 1034, 986, 903, 833 cm^{-1}. HRMS (ESI): *m/z* [M+H]$^+$ Calcd for $C_{15}H_{13}ClN_8O_3S$, 421.0598; Found, 421.0584.

4.3.2.3.2. Ethyl4-((4-chloro-6-(2-isonicotinoylhydrazinyl)-1,3,5-triazin-2 -yl) amino)benzoate (UHLMTJ-257b). Yield 83%. mp > 300 °C. ^{1}H NMR (DMSO-d_6): δ 10.99 (d, 1H, —NH——N**H**—C═O), 10.64 (brs, 1H, —N**H**—NH —C═O), 10.34 (brs, 1H, —N**H**), 8.82–8.76 (m, 2H, Ph—**H**), 7.90–7.77 (m, 4H, Py—**H**, Ph—**H**), 7.65 (d, J = 8.4 Hz, 2H, Py—**H**), 4.20–4.16 (q, 2H, —OC**H**$_2$—CH$_3$), 1.26 (t, J = 7.2, 3H, —C**H**$_3$). ^{13}C NMR (DMSO-d_6, 150.91 MHz) δ: 169.01, 167.63, 165.59, 164.96, 151.08, 143.43, 139.74, 130.52, 130.04, 124.48, 121.89, 120.01, 60.95, 14.61 ppm. IR (neat): ν_{max} 3281, 1688, 1605, 1539, 1508, 1411, 1366, 1276, 1227, 1176, 1107, 1017, 982, 901, 856 cm^{-1}. HRMS (ESI): *m/z* [M+H]$^+$ Calcd for $C_{18}H_{16}ClN_7O_3$, 414.1081; Found, 414.1078.

4.3.2.3.3. 4-((4-chloro-6-(2-isonicotinoylhydrazinyl)-1,3,5-triazin-2-yl)amino)benzenesulfonic acid (UHLMTJ-257c). Yield 72%. mp 300 °C. ^{1}H NMR (600 MHz, DMSO-d_6) δ 11.16 (brs, 1H, —N**H**—NH—C═O), 10.32 (d, 1H, —NH—N**H** —C═O), 9.98 (brs, 1H, —N**H**), 9.0–8.88 (m, 2H, Ph—**H**) 8.10–8.02 (m, 2H, Py—**H**), 7.53 (d, J = 8.4 Hz, 2H, Py—**H**), 7.40 (d, J = 8.4 Hz, 2H, Ph—**H**), 7.16 (brs, 1H, —O**H**). IR (neat): ν_{max} 3205, 1615, 1568, 1515, 1491, 1317, 1277, 1165, 1030, 984, 908, 834 cm^{-1}. HRMS (ESI): *m/z* [M+H]$^+$ Calcd for $C_{15}H_{12}ClN_7O_4S$ 422.0438, Found: 422.0431.

4.3.2.4. General procedure for synthesis of the target compound (UHLMTJ-258 a-c). To the solution of Dichloro substituted triazene **UHLMTJ-257a-c** (0.01 mol) and corresponding arylamine (0.02 mol) in dry acetic acid under N_2 conditions were reflexed at 110 °C for 1 h. After relaxation, the reaction mixture was cooled and into ice-cooled water, then was filtered to get a solid product. Finally, the compound was washed with hot water and hexane to get a required product, which was further crystallized with 1,4-dioxane.

4.3.2.4.1. 4-((4-(2-isonicotinoylhydrazinyl)-6-(p-tolylamino)-1,3,5-triazin-2-yl)amino)benzenesulfonamide (UHLMTJ-258a). Yield 80%. mp Infusible. ^{1}H NMR (600 MHz, DMSO-d_6): δ 10.74 (d, 1H, —NH—N**H**—C═O), 9.27 (brs, 1H, —N**H**), 8.80–8.74 (br, 2H, —N**H**-NH—C═O, —N**H**), 8.0–7.62 (m, 8H, Ph—**H,** Py—**H**), 7.50 (brs, 2H, —N**H**$_2$-S═O), 7.25–7.07 (m, 4H, Ph—**H**), 3.41 (**H**$_2$O), 24 (s, 3H, —C**H**$_3$). ^{13}C NMR (DMSO-d_6, 150.91 MHz) δ:167.94, 167.82, 164.81, 164.57, 150.98, 150.72, 140.31, 139.88, 137.10, 129.40, 126.84, 122.26, 121.97, 120.20, 119.55, 20.95 ppm. IR (neat): ν_{max} 3263, 1561, 1487, 1405, 1321, 1154, 1034, 1007, 985, 905, 833 cm^{-1}. HRMS (ESI): *m/z* [M+H]$^+$Calcd for $C_{22}H_{21}N_9O_3S$, 492.1566; Found, 492.1557.

4.3.2.4.2. Ethyl-4-((4-(2-isonicotinoylhydrazinyl)-6-(p-tolylamino)-1,3,5-triazin-2-yl) amino) benzoate (UHLMTJ-258b). Yield 87%. mp

238–240 °C. ^{1}H NMR (600 MHz, DMSO-d_6): δ10.75 (d, 1H, —NH—N**H**—C═O), 9.27–9.21 (br, 2H, —N**H**, —N**H**—NH—C═O), 8.80 (brs, 1H, —N**H**), 8.0–7.48 (m, 8H, Ph—**H,** Py—**H**), 7.12 (d, J = 6.6 Hz, 2H, Ph—**H**), 7.07 (d, J = 8.4 Hz, 2H, Ph—**H**), 4.26–4.22 (q, 2H, —C**H**$_2$–CH$_3$), 3.37 (**H**$_2$O), 2.24 (s, 3H, —C**H**$_3$), 1.26 (t, 3H, —CH$_2$–C**H**$_3$). IR (neat): ν_{max} 3267, 1571, 1486, 1407, 1364, 1273, 1173, 1104, 1033, 1008, 805 cm^{-1}**.** HRMS (ESI): *m/z* [M+H]$^+$ Calcd for $C_{25}H_{24}N_8O_3$, 485.2050; Found, 485.2047.

4.3.2.4.3. 4-((4-(2-isonicotinoylhydrazinyl)-6-(p-tolylamino)-1,3,5-triazin-2-yl) amino) benzenesulfonic acid (UHLMTJ-258c). Yield 68%. mp > 300 °C.^{1}H NMR (600 MHz, DMSO-d_6): δ11.01 (brs, 1H, —N**H**), 9.50 (d, 1H, —N**H**—N**H**—C═O), 9.40 (d, 1H, —N**H**—N**H**—C═O), 8.96 (m, 4H, Py—**H),** 8.09 (m, 4H, Ph—**H),** 7.70–7.45 (m, 3H, Ph—**H**, —N**H**), 7.08 (d, J = 8.4 Hz, 2H, Ph—**H),** 2.23 (s, 3H, —C**H**$_3$).—OH protan Exchange. IR (neat): ν_{max} 3291, 1556, 1488, 1407, 1325, 1171, 1123, 1032, 1006, 833 cm^{-1}. HRMS (ESI): *m/z* [M+H]$^+$ Calcd for $C_{22}H_{20}N_8O_4S$, 493.1406; Found, 493.1409.

4.3.2.5. General procedure for synthesis of the target compound (UHLMTJ-259 a-c). The monochloride substituted triazene, **7a-c** (0.01 mol), and the corresponding arylamine (0.01 mol) were dissolved in 1,4-dioxane at RT. During the reaction, the released HCl was neutralized with dropwise added 4% of NaOH (Alternatively, dry DMF as a solvent and K_2CO_3 as a neutralizing agent also used) and continue reaction up to 3 h and maintained reaction mixture at pH 7.5–8.0. After completing the reaction, the total blend was neutralized, washed with excess water, filtered to get the recrystallized product in dry DMF.

4.3.2.5.1. 4-((4-chloro-6-((4-(4-oxo-3-hydroquinazolin-2-yl)phenyl) amino)-1,3,5-triazin-2-yl)amino)benzene sulfonamide (UHLMTJ-259a). Yield 74%. mp Infusible. ^{1}H NMR (600 MHz, DMSO-d_6) δ 8.30 (brs, 1H, —N**H** = CO), 8.16 (d, J = 8.4 Hz, 2H,-Ph—**H**), 7.80–7.70 (m, 4H, Ph—**H**), 7.59 (d, J = 8.4 Hz, 2H, Ph—**H**), 7.50–7.41 (m, 2H, Ph—**H**), 7.27 (s, 2H, —N**H**$_2$-S═O), 7.23–7.20 (m, 2H, Ph—**H**), 6.73 (d, J = 8.4 Hz, 1H, Ph- H), 6.67–6.63 (m, 1H, Ph—**H**), 5.71 (s, 1H,- N**H**), 2.86 (DMF—**H**), One —NH protan Exchange. IR (neat): ν_{max} 3281, 1560, 1490, 1407, 1331, 1237, 1155, 1129, 1035, 1007, 988, 900, 832 cm^{-1}. HRMS (ESI) *m/z* [M+H]$^+$: Calcd for $C_{23}H_{17}ClN_8O_3S$, 521.0911; Found, 521.0909.

4.3.2.5.2. Ethyl 4-((4-chloro-6-((4-(4-oxo-3-hydroquinazolin-2-yl) phenyl)amino)-1,3,5-triazin-2-yl)amino)benzoate (UHLMTJ-259b). Yield 81%. mp 240–241 °C. ^{1}H NMR (600 MHz, DMSO-d_6) δ 8.26 (brs, 1H, —N**H** = CO), 7.95–7.80 (m, 8H, Ph —**H**), 7.58 (d, J = 6.6 Hz, 1H, Ph—**H**), 7.44 (d, 1H, Ph—**H**), 7.46–7.20 (m, 1H, Ph—**H**), 7.20 (d, J = 6.6 Hz, 1H, Ph—**H**), 6.62 (d, J = 6.6 Hz, 1H, Ph—**H**), 5.70 (brs, 1H, —N**H**), 4.24 (q, J = 7.2 Hz, 2H, —OC**H**$_2$—CH$_3$), 2.86 (DMF—**H**), 1.26 (t, J = 7.2 Hz, 3H, —C**H**$_3$), One —NH protan Exchange. IR (neat): ν_{max} 3287, 1566, 1487, 1409, 1365, 1309, 1274, 1240, 1175, 1107, 1017 cm^{-1}. HRMS (ESI): *m/z* [M+H]$^+$ Calcd for $C_{26}H_{21}ClN_7O_3$, 514.1394; Found, 514.1395.

4.3.2.5.3. 4-((4-chloro-6-((4-(4-oxo-3-hydroquinazolin-2-yl)phenyl) amino)-1,3,5-triazin-2 yl)amino)benzenesulfonic acid (UHLMTJ-259c). Yield 68%. mp > 300 °C, ^{1}H NMR (600 MHz, DMSO-d_6) δ 8.14–8.09 (brs, 2H, —N**H** = CO, —N**H**), 7.90–7.76 (m, 5H, Ph—**H**), 7.70–7.51 (m, 6H, Ph- **H**), 7.22–7.16 (m, 1H, Ph—**H**), 7.11 (s, 1H, —O**H),** One —NH protan Exchange**.** IR (neat): ν_{max} 3270, 1556, 1489, 1405, 1322, 1162, 1121, 1031, 1006, 986, 832 cm^{-1}. HRMS (ESI): *m/z* [M+H]$^+$ Calcd for $C_{23}H_{16}ClN_7O_4S$, 522.0751;Found, 522.0748.

4.3.2.6. General procedure for synthesis of the target compound (UHLMTJ-260 a-c, UHLMTJ-261 a-c). To the solution of dichloro substituted triazene **UHLMTJ-259 a-c** (0.01 mol) and corresponding arylamine (0.02 mol) in dry acetic acid under N_2 conditions were reflexed at 110 °C for 1 h. After relaxation, the reaction mixture was cooled and into ice-cooled water, then was filtered to get a solid product. Finally, the compound was washed with hot water and hexane to get a required product, which was further crystallized with 1,4-dioxane.

4.3.2.6.1. 4-((4-((4-(4-oxo-3-hydroquinazolin-2-yl) phenyl) amino)-6-(p-tolylamino)-1,3,5-triazin-2-yl) amino)benzenesulfonamide (UHLMTJ-260a). Yield 74%. mp 300 °C. ^{1}H NMR (600 MHz, DMSO-d_6): δ 9.66–9.22 (brs, 4H, all —N**H**, —N**H**—C═O), 8.16–7.95 (m, 4H, Ph—**H**), 7.80–7.43 (m, 8H, Ph—**H**), 7.25–7.10 (m, 6H, —N**H**$_2$-S═O, Ph—**H**), 3.34 (**H**$_2$O), 2.23 (brs, 3H, —C**H**$_3$). ^{13}C NMR (DMSO-d_6, 150.91 MHz) δ:164.61, 164.52, 164.33, 162.98, 152.57, 149.44, 143.71, 137.38, 135.08, 132.10, 129.60, 129.46, 129.36, 128.81, 127.85, 126.91, 126.68, 126.40, 126.14, 121.43, 121.24, 119.87, 119.67, 21.02 ppm. IR (neat): ν_{max} 3272, 2324, 205, 1914, 1603, 1566, 1538, 1486, 1400, 1320, 1247, 1151, 1095, 987, 833, 802 cm^{-1}. HRMS (ESI): *m/z* [M+H]$^+$ Calcd for $C_{30}H_{25}N_9O_3S$, 592.1879; Found, 592.1885.

4.3.2.6.2. Ethyl-4-((4-((4-(4-oxo-3-hydroquinazolin-2-yl)phenyl) amino)-6-(p-tolylamino)-1,3,5-triazin-2-yl)amino)benzoate (UHLMTJ-260b). Yield 78%. mp 258–260 °C. ^{1}H NMR (600 MHz, DMSO-d_6): δ10.1–9.0 (brs, 4H, all —N**H**, —N**H**—C═O), 8.20–7.39 (m, 14H, Ph—**H**), 7.20–7.05 (m, 2H, Ph—**H),** 4.25–4.18 (q, 3H, —C**H**$_2$), 2.25 (brs, 3H, —C**H**$_3$)0.1.22 (t, 3H, —C**H**$_3$). IR (neat):ν_{max}3272, 2350, 2285, 2112, 1981, 1916, 1681, 1614, 1567, 1556, 1514, 1487, 1455, 1403, 1214, 1169, 1120, 1031, 1006, 870, 836, 803 cm^{-1}. HRMS (ESI): *m/z* [M+H]$^+$ Calcd for $C_{33}H_{28}N_8O_3$, 585.2364; Found, 585.2367.

4.3.2.6.3. 4-((4-((4-(4-oxo-3-hydroquinazolin-2-yl) phenyl) amino)-6-(p-tolylamino)-1,3,5-triazin-2-yl) amino) benzenesulfonic acid (UHLMTJ-260c). Yield 65%. mp Infusible,^{1}H NMR (600 MHz, DMSO-d_6)**:**δ 9.9–9.3 (brs, 4H, all —N**H**, —N**H**—C═O) 8.30–8.08 (m, 2H, Ph—**H**), 7.82 (d, J = 8.4 Hz, 1H, Ph—**H**), 7.74–7.43 (m, 12H, Ph—**H**), 7.11 (d, J = 8.4 Hz, 1H,-Ph—**H**)6.8 (brs, 1H, —O**H**), 2.30 (s, 3H, —C**H**$_3$). IR (neat): ν_{max} 3291, 1557, 1486, 1405, 1324, 1164, 1121, 1031, 1005, 830 cm^{-1}. HRMS (ESI): *m/z* [M+H]$^+$ Calcd for $C_{30}H_{25}N_8O_4S$, 593.1719; Found, 593.1724.

4.3.2.6.4. 4-((4-(2-isonicotinoylhydrazinyl)-6-((4-(4-oxo-3-hydro-quinazolin-2-yl)phenyl)amino)-1,3,5-triazin-2-yl)amino)benzene sulfonamide (UHLMTJ-261a). Yield 79%. mp Infusible. ^{1}H NMR (600 MHz, DMSO-d_6): δ 10.84 (brs, 1H, —N**H**—N**H**—C═O), 8.77 (brs, 2H, —N**H**—C═O, —N**H**), 8.15 (m, 2H, Ph—**H**), 7.9–7.68 (m, 12H, Ph—**H,** Py—**H**, —N**H**$_2$-S═O), 7.45 (d, J = 6.6 Hz, 1H, Ph—**H**), 7.3–7.17 (m, 3H, Ph—**H**), two —NH protans are Exchange**.** IR (neat): ν_{max} 3287, 1556, 1486, 1407, 1327, 1228, 1155, 1035, 1008, 832 cm^{-1}. HRMS (ESI): *m/z* [M+H]$^+$ Calcd for $C_{29}H_{23}N_{11}O_4S$, 622.1733; Found, 622.1738.

4.3.2.6.5. Ethyl-4-((4-(2-isonicotinoylhydrazinyl)-6-((4-(4-oxo-3-hydroquinazolin-2-yl) phenyl) amino)-1,3,5-triazin-2-yl) amino) benzoate (UHLMTJ-261b). Yield 81%. mp 260–262 °C.^{1}H NMR (600 MHz, DMSO-d_6): δ 8.75 (brs, 2H, —N**H**—C═O, —N**H**), 8.16 (d, J = 8.4 Hz, 1H, Py—**H**), 8.10 (d, J = 8.4 Hz, 1H, Py—**H**), 8.0–7.82 (m, 12H, Ph—**H,** Py—**H**), 7.80–7.63 (m, 2H, Ph—**H**), 7.44 (brs, 1H, —N**H**), 4.25–4.22 (q, J = 8.4 Hz, 2H, —C**H**$_2$), 1.27 (t, J = 8.4 Hz, 3H, –C**H**$_3$) two —NH protans are Exchange. IR (neat): ν_{max} IR (neat): ν_{max} 3205, 1650, 1554, 1484, 1404, 1284, 1177, 1127, 1035, 981, 832, 800 cm^{-1}. HRMS (ESI): *m/z* [M+H]$^+$ Calcd for $C_{32}H_{26}N_{10}O_4$, 615.2217; Found, 615.2220.

4.3.2.6.6. 4-((4-(2-isonicotinoylhydrazinyl)-6-((4-(4-oxo-3-hydro-quinazolin-2-yl)phenyl)amino)-1,3,5-triazin-2-yl)amino)benzenesulfonic acid (UHLMTJ-261c). Yield 73%. mp Infusible. ^{1}H NMR (600 MHz, DMSO-d_6):δ 10.92 (brs, 1H, —NH—N**H**—C═O), 8.8 (brs, 2H, N**H**—C═O, —N**H**), 8.15–7.95 (m, 6H, Ph—**H,** Py—**H**), 7.88–7.37 (m, 10*H*, Ph—**H,** Py—**H**), 6.72 (brs, 1H, —O**H**), two —NH are Exchange. IR (neat): ν_{max} 3291, 1556, 1488, 1407, 1325, 1171, 1123, 1032, 1006, 833 cm^{-1}. HRMS (ESI): *m/z* [M+3H]$^+$ Calcd for $C_{29}H_{23}N_{10}O_5S$, 625.1730; Found, 625.1711.

5. Cell cytotoxicity by MTT assay

Cytotoxicity in SUP-T1 cells was measured by quantifying 3-(4,5-dimethylthiozol-2-yl) color change -2,5-diphenyltetrazolium bromide (MTT, Sigma) in the presence of different concentrations of the synthesized compounds and nanoparticles. According to the procedure, the

96-well plate was the seed with SUP-T1 cells at a density of $0.2x10^6$ cells/well and incubated at 37 °C in a 5% CO_2 incubator for 4 h. The incubated cells were treated with different concentrations of the synthesized compounds and nanoparticles. After treatment, the cells were again incubated for 16 h in the same incubation conditions. The cells were pelleted at 1200 rpm for 7 min and resuspended in complete medium. Now, 20 µl of 5 mg/ml pre-dissolved MTT was added to each well and incubated for another 4 h. After the incubation, the cells were pelleted at 1200 rpm for 10 min, discarded the media from wells, and formed MTT-formazan crystals were dissolved in DMSO by adding 100 µL into each well. Finally, the plate was incubated in the dark for 5 min, and the color change was recorded in an ELISA reader at 595 nm. The experiments were conducted in triplicate, and the average with standard deviation was plotted to represent the cell survival.

6. HIV-1 antiviral activity quantified by p24-ELISA assay

6.1. HIV-1 antiviral assay

10^6 SupT1 cells were suspended in RPMI 1640 supplemented with 0.1% FBS were seeded per well and followed by treatment with different concentrations of the synthesized compounds and nanoparticles. The compounds were added to the cells, followed by infection with 1 ng/ml p24 equivalent of 93IN101 and NL43 virus strains of clade C and clade B were used to study the inhibition by the molecules. The cells were incubated for 4 h at 37 °C in a 5% CO_2 incubator. After incubation, the cells were pelleted at 1200 rpm for 7 min, and the supernatant was discarded. The cells pellets were washed with fresh medium (RPMI 1640 supplemented with 10% FBS), resuspended in medium, and incubated for 96 h. After the incubation, the cells were pelleted down, and supernatants were collected for p24 antigen estimation as per the below described protocol. p24 levels in the absence of compounds were considered 0% inhibition and were taken as a negative control, and in the presence of known drugs T20 (Enfuvirtide) were considered positive control. Each experiment is conducted in triplicates; the data is presented as Mean ± Standard Deviation.

6.2. p24-ELISA assay

The HIV-1 core p24 antigen was collected from cell supernatent and quantified by p24 Antigen ELISA Kit after 96 h of incubation. The infection of the virus was quantified as on detected levels of viral antigen p24. The p24 quantification was followed as per the manufacturer's guidelines. The collected supernatants were diluted to 10-fold with complete media and then added 100 µl of the dilutions to each well of the pre-coated ELISA plate. To each well, 25 µl disruption buffer was added, and the plate was sealed. The plate was incubated for 1hr at 37 °C. After incubation, each well's contents were aspirated, and the wells were washed with wash buffer 3x times. Followed, 100 µl of the conjugate solution was added to each well, and again the plate was incubated for 1hr at 37 °C. After 1hr incubation, the solution was aspirated, and the plate was washed for 3x times, and then 100 µl of substrate solution was added to each well, and the pate was sealed. After incubation for 20 min at room temperature, the reaction was stopped by adding 100 µl of 1 N HCl. Finally, the plate was inserted into the ELISA reader and measured each well's optical density at 450 nm.

7. Inhibition of cell fusion

7.1. HL2/3 labelling

HL2/3 cells were incubated with 0.5 µM of Calcein AM for 1 h at 37 °C. After incubation, the cells were washed by spinning 350xg. After washing, the pellet was incubated for 30 min at 37 °C in fresh medium. The dye treated cells were incubated with compounds for 1 h after loading the dye.

7.2. SupT1 labelling

SupT1 cells were incubated with fluorescent dye Hoechst (20 µM) for 1 h at 37 °C. After incubation, the cells were pelleted at 350xg, and the pellet was resuspended in fresh medium and incubated another 30 min.

7.3. Dye redistribution assay

The fluorescent dye-labeled, Env protein-expressing cell line (HL2/3) and CD4+, CCR5+, CXCR4+ contained cell line (SupT1) were mixed co-cultured at a ratio of 1:1 and incubated at 37 °C for 2 h. The fusion was monitored at IC_{80} concentration of the compounds. The fusion in the presence of 50 nM of T20 was considered positive control and cells in absence of compounds is considered as negative control. After incubation, the extent of fused cells was observed using a Leica Fluorescent microscope or Leica Confocal microscope.

Funding

Research work is funded under DBT project BT/PR24076/Med/29/1210/2017. JS received funding through the University Grants Commission for doctoral fellowship and support. AB received funding through Indian Council of Medical Research for doctoral fellowship.

Declaration of Competing Interest

The authors declare that they have no known competing financial interests or personal relationships that could have appeared to influence the work reported in this paper.

Acknowledgement

The authors thank DBT, DST FIST, UGC SAP, UG UPE-II, DBT Builder program for providing central facilities. The authors thank ACRHEM, University of Hyderabad for support in spectroscopy experiments.

Appendix A. Supplementary material

Supplementary data to this article can be found online at https://doi.org/10.1016/j.bioorg.2021.105313.

References

[1] E. Crublet, J.-P. Andrieu, R.R. Vivès, H. Lortat-Jacob, The HIV-1 Envelope Glycoprotein gp120 Features Four Heparan Sulfate Binding Domains, Including the Co-receptor Binding Site, J. Biol. Chem. 283 (22) (2008) 15193–15200.
[2] R.B. Dennis, R.M. John, Antibody responses to envelope glycoproteins in HIV-1 infection, Nat. Immunol. 16 (6) (2015) 571–576.
[3] R.L. Stanfield, E. Cabezas, A.C. Satterthwait, E.A. Stura, A.T. Profy, I.A. Wilson, Dual conformations for the HIV-1 gp120 V3 loop in complexes with different neutralizing Fabs, Structure 7 (2) (1999) 131–142.
[4] Einat Schnur, Naama Kessler, Yuri Zherdev, Eran Noah, Tali Scherf, Fa-Xiang Ding, Svetlana Rabinovich, Boris Arshava, Victoria Kurbatska, Ainars Leonciks, Alexander Tsimanis, Osnat Rosen, Fred Naider, Jacob Anglister, NMR mapping of RANTES surfaces interacting with CCR5 using linked extracellular domains, FEBS J. 280 (9) (2013) 2068–2084.
[5] C.C. Huang, M. Tang, M.Y. Zhang, S. Majeed, E. Montabana, R.L. Stanfield, D. S. Dimitrov, B. Korber, J. Sodroski, I.A. Wilson, R. Wyatt, P.D. Kwong, Structure of a V3-containing HIV-1 gp120 core, Science 310 (5750) (2005) 1025–1028.
[6] X. Jiang, V. Burke, M. Totrov, C. Williams, T. Cardozo, M.K. Gorny, S. Zolla-Pazner, X.P. Kong, Conserved structural elements in the V3 crown of HIV-1 gp120, Nat. Struct. Mol. Biol. 17 (2010) 955–961.
[7] Phanourios Tamamis, Christodoulos A. Floudas, Emanuele Paci, Molecular recognition of CCR5 by an HIV-1 gp120 V3 loop, PLoS ONE 9 (4) (2014) e95767, https://doi.org/10.1371/journal.pone.009576710.1371/journal.pone.0095767.g00110.1371/journal.pone.0095767.g00210.1371/journal.pone.0095767.g00310.1371/journal.pone.0095767.t00110.1371/journal.pone.0095767.s00110.1371/journal.pone.0095767.s00210.1371/journal.pone.0095767.s00310.1371/journal.pone.0095767.s00410.1371/journal.pone.0095767.s00510.1371/journal.pone.0095767.s00610.1371/journal.pone.0095767.s00710.1371/journal.pone.0095767.s00810.1371/journal.pone.0095767.s00910.1371/journal.pone.0095767.s01010.1371/journal.pone.0095767.s01110.1371/journal.pone.0095767.s01210.1371/journal.pone.0095767.

s01310.1371/journal.pone.0095767.s01410.1371/journal.pone.0095767.s01510.1371/journal.pone.0095767.s01610.1371/journal.pone.0095767.s01710.1371/journal.pone.0095767.s01810.1371/journal.pone.0095767.s01910.1371/journal.pone.0095767.s02010.1371/journal.pone.0095767.s021.

[8] J.M. Rini, R.L. Stanfield, E.A. Stura, P.A. Salinas, A.T. Profy, I.A. Wilson, Crystal structure of a human immunodeficiency virus type 1 neutralizing antibody, 50.1, in complex with its V3 loop peptide antigen, Proc. Natl. Acad. Sci. USA 90 (13) (1993) 6325–6329.

[9] (i) K. April, Z. Hui-Tang, S. Brett, W. Constance, K.G. Miroslaw, Z.P. Susan, K. Xiang-Peng, Thermodynamic Signatures of the Antigen Binding Site of mAb 447−52D Targeting the Third Variable Region of HIV–1 gp120, Biochemistry 52 (2013) 6249−6257; (ii) P. Acharya, C. Dogo-Isonagie, J.M. Lalonde, S.N. Lam, G.J. Leslie, M.K. Louder, L.L. Frye, A.K. Debnath, J.R. Greenwood, T.S. Luongo, et al., Structurebased identification and neutralization mechanism of tyrosine sulfate mimetics that inhibit HIV-1 entry, ACS Chem. Biol. 6 (2011) 1069–1077.

[10] V. Burke, C. Williams, M. Sukumaran, S.S. Kim, H. Li, X.H. Wang, M.K. Gorny, S. Zolla-Pazner, X.P. Kong, Structural Basis of the Cross-Reactivity of Genetically Related Human Anti-HIV-1 mAbs: Implications for Design of V3-Based Immunogens, Structure. 17 (2009) 1538–1546.

[11] R.L. Stanfield, M.K. Gorny, C. Williams, S. Zolla-Pazner, I.A. Wilson, Structural Rationale for the Broad Neutralization of HIV-1 by Human Monoclonal Antibody 447–52D, Structure. 12 (2004) 193–204.

[12] K.D. Amandeep, L.S. Robyn, K.G. Miroslaw, W. Constance, Z.P. Susan, A.W. Ian, Structure determination of an anti-HIV-1 Fab 447–52D–peptide complex from an epitaxially twinned data set, Acta Cryst. D 64 (2008) 792–802.

[13] A.D. Lawson, Antibody-enabled small-molecule drug discovery, Nat. Rev. Drug Discovery 11 (2012) 519.

[14] H.H. Refsgaard, B.F. Jensen, P.B. Brockhoff, S.B. Padkjaer, M. Guldbrandt, M. S. Christensen, *In silico* prediction of membrane permeability from calculated molecular parameters, J. Med. Chem. 48 (3) (2005) 805–811.

[15] B. Viira, A. Selyutina, A.T. García-Sosa, M. Karonen, J. Sinkkonen, A. Merits, U. Maran, Design, discovery, modelling, synthesis, and biological evaluation of novel and small, low toxicity s-triazine derivatives as HIV-1 non-nucleoside reverse transcriptase inhibitors, Bioorg. Med. Chem. 24 (11) (2016) 2519–2529.

[16] L. Lu, Y. Fei, C. Lifeng, K.D. Asim, J. Shibo, Development of Small-molecule HIV Entry Inhibitors Specifically Targeting gp120 or gp41, Curr. Top. Med. Chem. 16 (10) (2016) 1074–1090.

[17] S. Einat, K. Naama, Z. Yuri, N. Eran, S. Tali, D. Fa-Xiang, R. Svetlana, A. Boris, K. Victoria, L. Ainars, T. Alexander, R. Osnat, N. Fred, A. Jacob, NMR mapping of RANTES surfaces interacting with CCR5 using linked extracellular domains, FEBS J. 280 (9) (2013) 2068–2084.

[18] E.G. Cormier, M. Persuh, D.A. Thompson, S.W. Lin, T.P. Sakmar, W.C. Olson, T. Dragic, Specific interaction of CCR5 amino-terminal domain peptides containing sulfotyrosines with HIV-1 envelope glycoprotein gp120, PNAS 97 (2000) 5762–5767.

[19] C.A.M. Afonso, N.M.T. Lourenco, A.D.A. Rosatella, Synthesis of 2,4,6-Tri-substituted1,3,5-Triazines, Molecules 11 (2006) 81–102.

[20] N.C. Desai, H.M. Atul, R.D. Senta, Synthesis, characterization and antimicrobial activity of some new 4-(4-(2-isonicotinoylhydrazinyl)-6-((aryl)amino)-1,3,5-triazin-2-ylamino)-N-(pyrimidin-2-yl) benzenesulfonamides, Journal of Saudi Chemical Society. 21 (2017) S25–S34.

[21] Khadijah M. Al-Zaydi, Hosam H. Khalil, Ayman El-Faham, Sherine N. Khattab, Synthesis, characterization, and evaluation of 1,3,5–triazine aminobenzoic acid derivatives for their antimicrobial activity, Chem. Cent. J. 11 (2017) 39.

[22] S. Moni, C. Kuldeep, S. Rahul, V. Preeti, K.S. Manish, S. Abhisheak, G. Suman, K. S. Jitendra, L. Jawahar, C. Preeti, K. Brijesh, M. Prem, S. Chauhan, Discovery of a New Class of Natural Product-Inspired Quinazolinone Hybrid as Potent Antileishmanial agents, J. Med. Chem. 56 (2013) 4374–4392.

[23] S.K. Corey, M.S. Shaun, Rapid and convenient conversion of nitroarenes to anilines under microwave conditions using nonprecious metals in mildly acidic medium, Synth. Commun. 47 (11) (2017) 1085–1089.

[24] A.K. Kirill, An Efficient, "Green" Approach to Aryl Amination of Cyanuric Chloride Using Acetic Acid as Solvent, J. Heterocyclic Chem. 45 (2008) 533.

[25] L.R. Hollingsworth IV, A.M. Brown, R.D. Gandour, D.R. Bevan, Computational study of HIV gp120 as a target for polyanionic entry inhibitors: Exploiting the V3 loop region, PLoS ONE 13 (1) (2018), e0190658.

[26] D. Bowder, H. Hollingsead, K. Durst, D. Hu, W. Wei, J. Wiggins, H. Medjahed, A. Finzi, J. Sodroski, S.H. Xiang, Contribution of the gp120 V3 loop to envelope glycoprotein trimer stability in primate immunodeficiency viruses, Virology 521 (2018) 158–168.